Transmission spectra of single ring coupled-waveguide resonator configuration by finite difference time domain method

Haryana bin Mohd Hairi[1], Saktioto[2], Romi Fadli Syahputra[3], Okfalisa[4], Sofia Anita[5]
[1]Faculty of Applied Sciences, Universiti Teknologi MARA, Malaysia
[2,3]Faculty of Mathematics and Natural Sciences, Universitas Riau, Indonesia
[4]Science and Technology Faculty, Universitas Islam Negeri Sultan Syarif Kasim, Indonesia
[5]Department of Chemistry, Math and Natural Sciences Faculty, Universitas Riau, Indoensia

Article Info

Article history:

Received Mar 6, 2019
Revised Apr 16, 2020
Accepted May 1, 2020

Keywords:

Finite difference time domain
Microring
Power distribution
Resonator

ABSTRACT

Development of optical waveguide resonators have greatly expanded and continues to grow since they have kinds potential applications such as wavelength filtering, switching, coupling and multiplexing. One of resonators, coupled waveguides, ring resonators are designed and operated using various coupling configurations. Ring resonators can be particularly used as wavelength filter if the wavelength can fit a whole multiple time in the circumference of the ring. This article proposes to investigate the transmission spectra from the power source and amplify it in linearized ring resonator configurations and varies the input amplitude on five different wavelengths. With finite difference time domain method, the geometry and power source are simulated to obtain the better result and configuration. The results show the intensity phenomena of filtering in optical circuit.

This is an open access article under the CC BY-SA license.

CC BY SA

Corresponding Author:

Saktioto,
Department of Physics,
Faculty of Mathematics and Natural Sciences,
Universitas Riau,
Bina Widya Campus, Jl. HR Soebrantas KM 12.5, Pekanbaru, Riau, Indonesia.
Email: saktioto@yahoo.com, saktioto@lecturer.unri.ac.id

1. INTRODUCTION

Nowadays, the role of optical ring resonator has been widely used in photonic network, communication and kinds industrial application. It also has represented as the most promising optical circuit and photonic integration platforms. The basic ring resonator consists of a straight waveguide coupled to a fiber ring with radius, *r* [1-5]. A generic ring resonator consists of geometry symmetry, optical waveguide and dielectric structure which are looped back on it, such that a resonance system occurs when the optical path length of the resonator is exactly a whole number of wavelengths [6].

The finite difference time domain (FDTD) method is commonly used in solving Maxwell equations. This is proved to be one of the important tools due to its simple implementation in software simulations. This mathematical method was used in a variety of photonics' studies. By using FDTD method, Hagness et al. In [7] described the design and experimental realization of a simple ring resonator [6]. Modeling micro ring resonator is important due to the optical device offer a large free spectral range but also a narrow band [7, 8]. It is similar to fiber Bragg grating (FBG) [9-12], micro ring resonator has been proposed to biosensor applications [13], such as for Alzheimer diagnosis [14]. Perception of 3D image also can be built by micro ring resonator. This 3D view is obtained by Panda ring arrangement [15, 16]. However, some existing ring resonator designs have not been able to solve the problem of more complex wave intensity propagation in an optical circuit including also increasing the output power [17]. For this reason, it is necessary to design a simulation for several considerations and adjustments in optical circuits that are still required.

In this study we simulated linearized ring resonator configurations and vary the input amplitude on various wavelengths. The effect of input amplitude to power amplification for all configurations is evaluated and also varied to the input amplitude on different resonant wavelengths. It is necessary to analyze the effect of structures on ring resonator [18, 19] since power can be distributed while propagating through the structure for various performances. The output pattern of optical filter will vary due to particular orientation. Furthermore, it can be optimized the profile of the output waves.

2. RESEARCH METHOD

This research represents a model of resonator configuration commencing by setting up the wafer dimensions to 60 μm in length and 20 μm in width. The 2D wafer's refractive index set to air's refractive index which is 1.00. The waveguide being used to model this simulation is to set the isotropic constant refractive index which is its real value of 1.54 and no imaginary part. The device configuration is composed by a ring resonator and a plane waveguide as shown in Figure 1. The details of the configuration are as follows; the length of the linear waveguide has been set to 60.0 μm and the width of fiber is 1.0 μm. The waveguide is then coupled to double ring waveguide with radius of 3.25 μm, both minor and major radius. The centers of the horizontal position for the upper and lower rings are located at approximately at 8 until 50 μm by difference of 22 μm between each other. While the vertical position of the upper ring is approximately 4.1 μm and the vertical position are about -4.1 μm. The orientation angle of each ring waveguide is set to 0°. In this model, the default setting is used for the configuration of channel thickness tapering. The width of the ring is set to 1.0 μm and the depth is set similar to profile of plane waveguide. The vertical input plane is interfaced to the device as a power source. A continuous wave with wavelength of 1.55 μm has been used as the initial properties of the input plane for the Gaussian input field transverse. The plane geometry is set and wave configuration is 0.4 μm for its Z position being transverse in positive direction with 0° initial phase and the input power is 1.0V/m.

Electromagnetically, as the electric field propagates along the ring resonator, the fundamental relations amongst the incident field, E_1, transmitted field, E_2, and circulating fields E_3, E_4 of a single resonator are inferred by combining the relations for the coupler with that of the feedback path [8]. In the spectral domain as depicted in Figure 2, the electric field propagates to the the coupling region corresonding to the source of field through the subsequent unitary matrix is given by;

$$\begin{pmatrix} E_4(\omega) \\ E_2(\omega) \end{pmatrix} = \begin{pmatrix} r & it \\ it & r \end{pmatrix} \begin{pmatrix} E_3(\omega) \\ E_1(\omega) \end{pmatrix} \tag{1}$$

where the lumped self- and cross-coupling coefficient, r and t are assumed to be autonomous of frequency and fulfill the relations of $r^2 + t^2 = 1$ [8]. If the feedback path (of length, $2\pi R$) connects the output from port 4 backward into input port 3 where the electric field is stated by

$$E_3 = exp(-\pi\alpha_{ring}R)\, exp(2i\pi kR) = a\, exp(\,i\phi)E_4 \tag{2}$$

The value of a represents the single-pass amplitude transmission and ϕ is the single-pass phase shift. In (1) and (2) are solved to obtain the solution of for the ratio of the circulating field to the electric field incident;

$$\frac{E_3}{E_1} = \frac{ita\, exp(i\phi)}{1-ra\, exp(i\phi)} \tag{3}$$

The ratio of the circulating intensity to the source of incident intensity, or the buildup factor $\mathcal{B}$, defined by the squared modulus of the results as (4).

$$B = \frac{I_3}{I_1} = \left|\frac{E_3}{E_1}\right|^2 = \frac{(1-r^2)a^2}{1-2ra\cos\varphi + r^2a^2} \tag{4}$$

The last outcomes may allude to the circumstance in which the incident intensity is resonant with the ring ($\emptyset = m2\pi$) where the losses or attenuation are not considered ($a = 1$). This passive ring resonator under these conditions obtains the maximum ratio of circulating power to incident power. For cross-coupling values of 10% ($t^2 = 0.1$), the intensity in the ring can be 40 times higher than the intensity incident on the resonator in the input waveguide. Based on the intensity in the optical ring resonator that can be higher than that of in the bus, ring resonator can be utilized for other optic applications and nonlinear ones with moderate input intensities [5].

Figure 1. The schematic diagram of ring resonator configuration

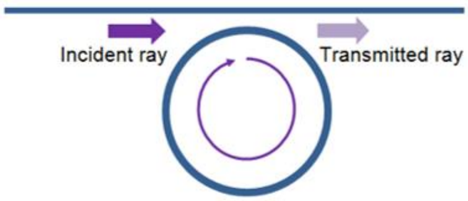

Figure 2. Electric field correlates with an all-pass ring resonator

3. RESULTS AND ANALYSIS

3.1. Single ring resonator and linear waveguide

Figure 3 describes results of light intensity before and after propagating the ring structure of single ring resonator. This study is conducted by five various wavelengths; λ=1.0 μm, λ=1.25 μm, λ=1.55 μm, λ=2.9 μm, λ=4.25 μm and the input power is set at V/m. Based on the results, from Figure 3 (a) it is found that the trend line is nearly symmetric at wavelength from 0.9 μm until 1.1 μm and a peak is found to rise at λ=1.0μm. There seems that the filter rises gradually and the gain is high at this range. Figure 3 (b) describes that the trend line is not symmetric compared in Figure 3 (a). The filter is slightly exponential and the gain is high but the wavelength filter is short to be used in practical application as an optical filter [19]. Figure 3 (c) shows that the peak at wavelength 1.55 μm is sharp and this produces a good filter in optical waveguide application. Besides, it depicts a comb wave rapidly and the gain is relatively high at this range compared in Figures 3 (a) and (b). As we increased the value of λ until 2.9 μm and 4.2 μm, it was found that the value of output power is less compared to input power which being supplied to the system shown in Figures (d) and (e). Contrary to expectation, it is assumed that the power is being reticulated as it propagates through the ring structure [6].

3.2. Input amplitude of 1 V/m, 5 V/m and 10 V/m

Figure 4 depicts that the higher input amplitude produces the narrower band wave as this one of the ideal characteristics for an optical filter of λ=1.55 μm. However, at higher input amplitude, we cannot clearly observe the gap between the input source and output source compared to the lower input amplitude. It is evident from the results; the trend line for various setting of input amplitude is similar to 1 V/m, 5 V/m and 10 V/m. These findings suggest that the power gain is generally good until it reaches λ=1.55 μm. At 2.9 μm, the output power is 90° to 180° phase difference due to power delays although power amplification is high [16]. As we increased the value of λ, they cannot act as a good optical filter since it has wide broadband. For lower value of λ, it can filter certain required wavelength since the peak is steep at certain range compared to bigger λ. These are due to the factor of higher wavelength carries high power energy [20]. Four serial-single ring resonators is a good filter compared to single ring resonator. However, the double ring resonator shows the sharp peak results. When increasing the input amplitude 1-10 V/m, the effect of phase difference and group velocity affect the filter wave profile mainly at high wavelength source [21]. The gain is sharp but for high input voltage the wave seems not sinusoidal, it suspects due to the effects of ring cannot completely acts as the resonator since several geometrical parameters are changed. It is the effect of nonlinear phenomena occurring in the light wave as it propagates through the bus and ring structure.

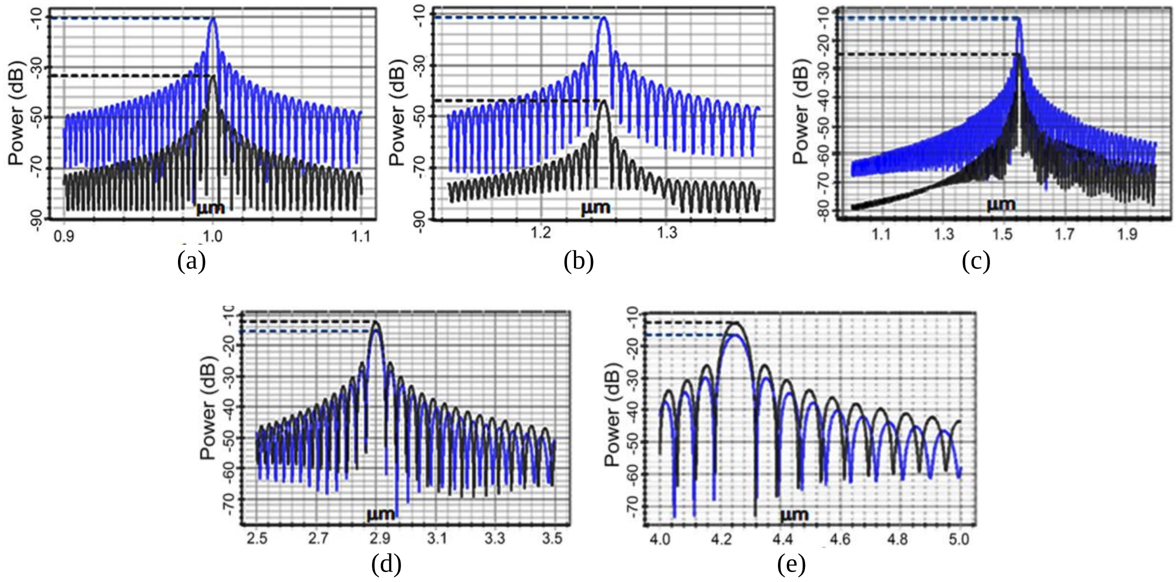

Figure 3. The transmission spectrum of single ring resonator with input amplitude of 1V/m; (a) at λ=1.0 µm, (b) at λ=1.25 µm, (c) at λ=1.55 µm, (d) at λ= 2.9 µm and (e) at λ= 4.25 µm. Horizontal line indicates wavelength in µm

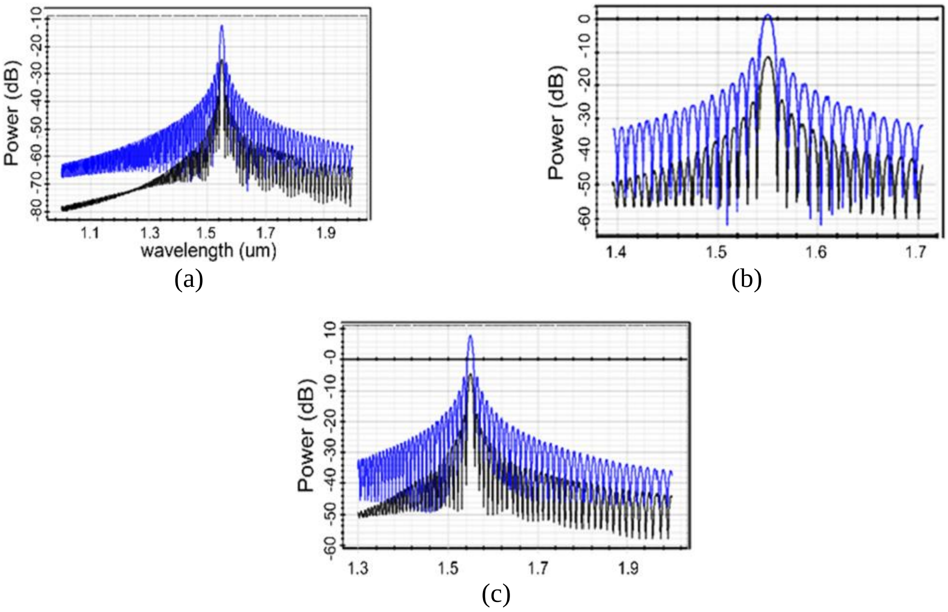

Figure 4. The transmission spectrum for single ring resonator for λ = 1.55 µm with (a) input amplitude of 1 V/m, (b) 5 V/m and (c) 10 V/m

3.3. Power amplification of light for linearized-double ring resonator

Figure 5 shows the power amplification for optical light in linearized-double ring resonator if it is evaluated the input amplitude of 1-10 V/m for wavelength range from 1 until 4.25 µm, as depicted in the curves, the dot lines and dashed lines represent the model and demonstration data respectively. These phenomena occur due to time delay when the light propagates in the ring [22], hence the energy losses are produced as it circulates in the ring. Furthermore, during the wave propagates in a circulation ring, there are phase difference due to time delay between the first and the next wave. For a larger wavelength, it carries low energy and it requires longer period to circulate in the ring [23]. Therefore, the higher wavelength sources as inversely proportional to frequency are able to reduce energy losses along the circulation and propagation in optical media [16, 22]. In future works, it is necessary to establish a relationship filtering phenomenon in micro ring resonator and metamaterial ring resonator [24-26].

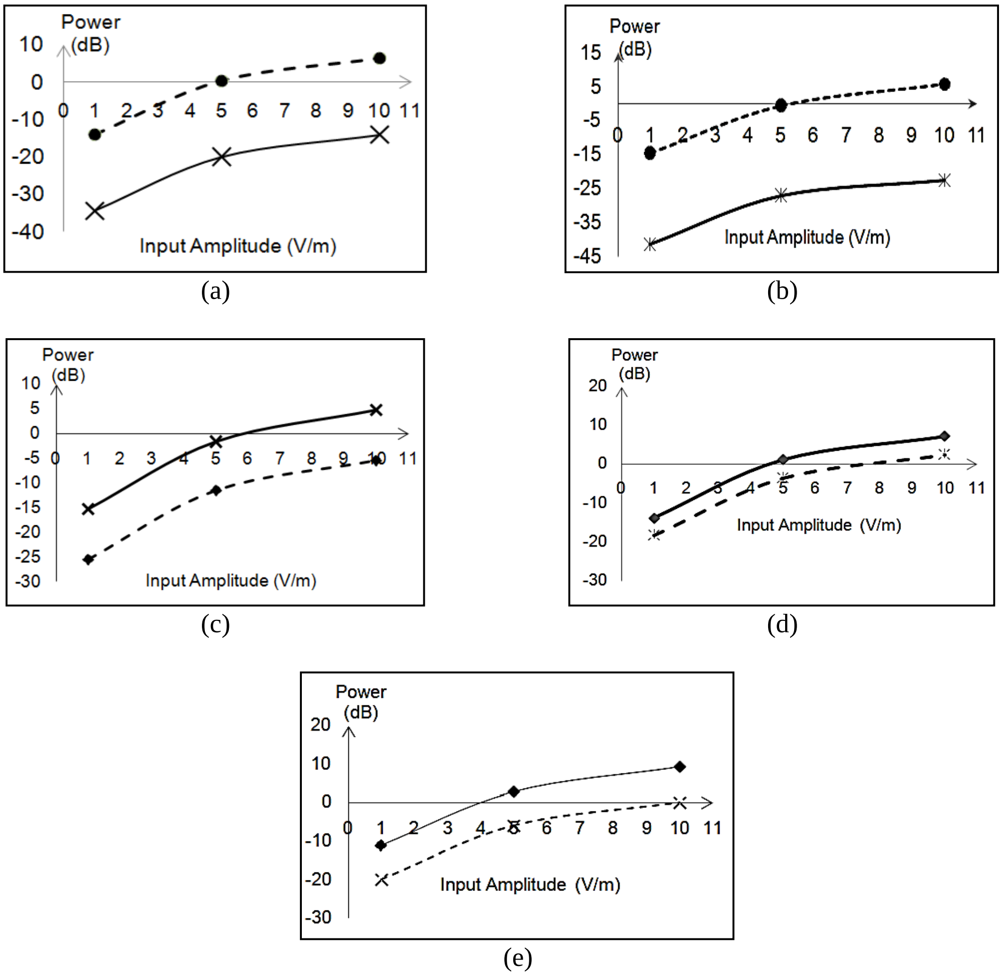

Figure 5. The power amplification of light intensity for double ring resonator;
(a) at λ = 1.0 µm, (b) 1.25 µm, (c) 1.55 µm, (d) 2.9 µm and (e) 4.25 µm

4. CONCLUSION

Numerical demonstration to design ring resonator and the influence of power sources in linearized coupled-ring resonator have been successfully investigated. This was commenced to the analysis of a single bus ring coupled with another resonator. It shows that the graph at wavelength of 1550 nm, the transmission spectrum from the output port at this specific wavelength is sharp and this produces it a good filter in optical waveguide application. After that, the effect of various input amplitude for λ = 1.55 µm reveals that the higher input amplitude produces, the narrower band wave is released, as this one of the important characteristics for an optical filter. However, if we increase the input energy, it is uneasy describes the gap between input and output optical spectrum. These are also compared to the transmission spectrum of double-ring configurations to identify the optimum that match to fulfill the ideal optical filter.

ACKNOWLEDGEMENTS

We would like to thank The Ministry of Research, Technology and BRIN, Indonesia for generous support of research Grant in 2020. We also thank Department of Physics, Math and Natural Sciences Faculty, Universitas Riau, Pekanbaru Indonesia for providing research facilities and Faculty of Applied Sciences, Universiti Teknologi MARA, Johor and University of Riau in collaborating research with a simulation method.

REFERENCES

[1] R. Orta, P. Savi R. Tascone and D. Trinchero, “Synthesis of multiple-ring-resonator filters for optical sytem,” *IEEE Photonics Technology Letters,* vol. 7, pp. 1447-1449, 1995.
[2] D. G. Rabus, “Integrated Ring Resonator: The Compendium,” *Heidelberg: Springer-Verlag*, 2007.
[3] W. Bogaerts, P. Dumon, D. Thourhout, D. Taillaert, P. Jaenen, J. Wouters, S. Beckx, V. Wiaux and R. Baets, “Compact wavelength-selective functions in silicon-on-insulator photonics wires,” *IEEE Journal of Selected Topics in Quantum Electronics*, vol. 12, no. 6, pp. 1394-1401, 2006.
[4] P. Dumon, W. Bogaerts, V. Wiaux, J. Wouters, S. Beckx, J. van Campenhout, D. Taillaert, B. Luyssaert, P. Bientsman, D. van Thourhout and R. Baets, “Low-loss SOI photonics wires and ring resonators fabricated with deep UV lithography,” *IEEE Photonics Technology Letters*, vol. 16, no. 5, pp. 1328-1330, 2004.
[5] J. Heebner, R. Grover and T. A. Ibrahim, “Optical Microresonator: Theory, Fabrication and Application,” *New York: Springer-Verlag*, pp. 74-77, 2008.
[6] W. Bogaerts, P. D. Heyn, T. V. Vaerenbergh, K. D. Vos, S. K. Selvaraja, T. Claes, P. Dumon, P. Bientsman, D. V. Thourhout and R. Baets, “Silicon microring resonator,” *Laser and Photonics Reviews*, vol. 6, no. 1, pp. 47-73, 2012.
[7] S. C. Hagness, D. Rafizadeh, S.T. Ho and A. Taflove, “FDTD Microcavity Simulations: Design and Experimental Realization of Waveguide-Coupled Single Mode Ring and Whispering-Gallery-Mode Disk Resonators,” *Journal of Lightwave Technology*, vol. 15, no. 11, pp. 2154-2165, 2007.
[8] W. Khunnam, J. Ali, I. S. Amiri F. H. Suhailin, G. Singh, P. Yupapin and K. T. V. Grattan, “Mode-locked self-pumping and squeezing photons model in a nonlinear micro-ring resonator,” *Optical and Quantum Electronics,* vol. 50, 2018.
[9] S. Sridevi, K. S. Vasu, S. Asokan and A. K. Sood, “Sensitive detection of C-reactive protein using optical fiber Bragg gratings,” *Biosensors and Bioelectronics*, vol. 65, pp. 251-256, 2015.
[10] R. F. Syahputra, Saktioto, R. Meri, Syamsudhuha and Okfalisa, “Profile of single mode fiber coupler combining with Bragg grating,” *TELKOMNIKA Telecommunication, Computing, Electronics and Control*, vol. 15, no. 3, pp. 1103-1107, 2017.
[11] S. M. Lee, S. S. Saini and M. Y. Jeong, “Simultaneous measurement of refractive index, temperature, and strain using etched-core fiber Bragg grating sensors,” *IEEE Photonics Technology Letters*, vol. 22, no. 19, pp. 1431-1433, 2010.
[12] A. K. Sarkaleh, B. V. Lahijani, H. Saberkari and A. Esmaeeli, “Optical Ring Resonators: A Platform for Biological Sensing Applications,” *Journal of Medical Signals and Sensors*, vol. 7, no. 3, pp. 185-191, 2017.
[13] C. Li, R. Zhao, J. Tang, M. Xia, H. Guo, C. Xie, L. Wang and J. Liu, “Erbium-doped fiber ring resonator for resonant fiber optical gyro applications,” *Optics Communications*, vol. 412, pp. 127-133, 2018.
[14] D. Irawan, T. Saktioto, J. Ali and P. Yupapin, “Design of Mach-Zehnder Interferometer and Ring Resonator for Biochemical Sensing,” *Photonic Sensors*, vol. 5, pp.12-18, 2015.
[15] T. Saktioto, D. Irawan, P.P. Yupapin and P. Phatharacorn, “A Single Eye 3D Image Perception Device using Vertical Double Ring Resonator Construction,” *Microwave and Optical Technology Letters*, vol. 57, no. 8, pp. 1802-1805, 2015.
[16] S. W. Huang, J. Yang, S. H. Yang, M. Yu, D. L. Kwong, T. Zelevinsky, M. Jarrahi and C. W. Wong, “Globally Stable Microresonator Turing Pattern Formation for Coherent High-Power THz Radiation On-Chip,” *Physical Review X*, 2017.
[17] X. Wang, J. Wang, S. Wang, H. Yang and Y. Liao, “Spectrum analysis of seawater and gasoline by microfiber ring resonator,” *Guangxue Xuebao/Acta Optica Sinica*, vol. 34, 2014.
[18] M. Aamer, A.M. Gutiérrez, A. Brimont and P. Sanchis, “Ring resonator structures for active applications in Silicon,” *Optica Pura y Aplicada*, vol. 45, no. 2, pp. 169-175, 2012.
[19] M. Bahadoran and I. S. Amiri, “Double critical coupled ring resonator-based add–drop filter," *Journal of Theoretical and Applied Physics*, vol. 13, pp. 213--220, 2019.
[20] H. Zhang, L. Zhou, J. Xu, L. Lu, J. Chen and B.M. Rahman, “All-optical non-volatile tuning of an AMZI-coupled ring resonator with GST phase-change material,” *Optics Letters*, vol. 43, no. 22, pp. 5539-5542, 2018.
[21] E. Dulkeith, F. Xia, L. Schares, W.M.J. Green and Y.A. Vlasov, “Group index and group velocity dispersion in silicon-on-insulator photonic wires,” *Optics Express*, vol. 14, no. 19, pp. 3853- 3863, 2006.
[22] T. Dai, A. Shen, G. Wang, Y. Wang, Y. Li, X. Jiang and J. Yang, “Bandwidth and wavelength tunable optical passband filter based on silicon multiple microring resonator,” Optics Letters, vol. 41, no. 20, pp. 4807-4810, 2016.
[23] G. K. Bharti, U. Biswas and J. K. Rakshit, “Design of micro-ring resonator based all optical universal reconfigurable logic circuit,” Optoelectronics and Advanced Materials, vol. 13, no. 7-8, pp. 407-414, 2019.
[24] T. Saktioto, R.F. Syahputra, S. Punthawanunt, J. Ali and P. Yupapin, “GHz frequency filtering source using hexagonal metamaterial splitting ring resonators,” *Microwave and Optical Technology Letters*, vol. 59, no. 6, pp. 1337-1340, 2017.
[25] S.K. Patel, S. Lavadiya, Y.P. Kosta, M. Kosta, T.K. Nguyen and V. Dhasarathan, “Numerical investigation of liquid metamaterial-based superstrate microstrip radiating structure,” *Physica B: Condensed Matter*, vol. 585, 2020.
[26] H. A. Atallah, “Design of metamaterial-based bandstop filters using complementary split ring resonators,” *International Journal of Advanced Science and Technology*, vol. 28, no. 16, pp. 1730-1739, 2019.